BIOCHEMISTRY
including biophysical chemistry & molecular biology

Article

pubs.acs.org/biochemistry

The Distal Helix in the Regulatory Domain of Calcineurin Is Important for Domain Stability and Enzyme Function

Tori B. Dunlap, Erik C. Cook, Julie Rumi-Masante, Hannah G. Arvin, Terrence E. Lester, and Trevor P. Creamer*

Center for Structural Biology, Department of Molecular and Cellular Biochemistry, University of Kentucky, 741 South Limestone Street, Lexington, Kentucky 40536-0509, United States

ABSTRACT: Calcineurin (CaN) is a calmodulin-activated, serine/threonine phosphatase that is necessary for cardiac, vasculature, and nervous system development, as well as learning and memory, skeletal muscle growth, and immune system activation. CaN is activated in a manner similar to that of the calmodulin (CaM)-activated kinases. CaM binds CaN's regulatory domain (RD) and causes a conformational change that removes CaN's autoinhibitory domain (AID) from its catalytic site, activating CaN. In the CaM-activated kinases, the CaM binding region (CaMBR) is located just C-terminal to the AID, whereas in CaN, the AID is 52 residues C-terminal to the CaMBR. Previously published data have shown that these 52 residues in CaN's RD are disordered but approximately half of them gain structure, likely α-helical, upon CaM binding. In this work, we confirm that this increase in the level of structure is α-helical. We posit that this region forms an amphipathic helix upon CaM binding and folds onto the remainder of the RD:CaM complex, removing the AID. Förster resonance energy transfer data suggest the C-terminal end of this distal helix is relatively close to the N-terminal end of the CaMBR when the RD is bound by CaM. We show by circular dichroism spectroscopy and thermal melts that mutations on the hydrophobic face of the distal helix disrupt the structure gained upon CaM binding. Additionally, kinetic analysis of CaN activity suggests that these mutations affect CaN's ability to bind substrate, likely a result of the AID being able to bind to the active site even when CaM is bound. Our data demonstrate the presence of this distal helix and suggest it folds onto the remainder of the RD:CaM complex, creating a hairpinlike chain reversal that removes the AID from the active site.

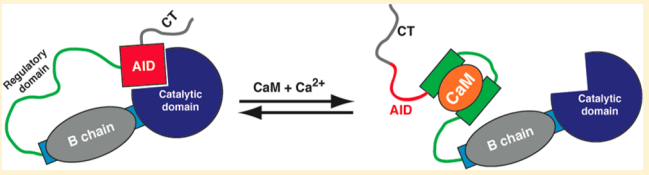

The calcium signaling protein calmodulin (CaM) is important in numerous signaling pathways and is known to have approximately 300 binding targets.[1] Among these targets are calmodulin-activated kinases such as CaM kinase I (CaMKI), CaM kinase II (CaMKII), CaM kinase kinase (CaMKK), and myosin light chain kinase (MLCK).[2] CaM-activated kinases possess an autoinhibitory domain (AID) that occludes the catalytic site, rendering the kinase inactive. When cellular calcium levels increase, CaM binds calcium ions and then binds the kinase at a site just C-terminal to the AID, the CaM binding region (CaMBR), causing a conformational change that removes the AID from the catalytic site, activating the kinase (Figure 1).[3]

In contrast to the CaM-activated kinases, there is only one known CaM-activated phosphatase, the serine/threonine phosphatase calcineurin (CaN).[4−6] CaN is involved in several developmental processes, including formation of the cardiac, vasculature, and nervous systems.[7] CaN is also necessary for learning and memory, skeletal muscle growth, and immune system activation.[7] As such, inappropriate CaN regulation has been implicated in pathological states such as Alzheimer's disease,[8] Down syndrome,[9] and cardiac hypertrophy.[10,11] Arguably, CaN's most well-known target is the nuclear factor of activated T-cells (NFAT) family of transcription factors.[7] CaN dephosphorylation of NFAT reveals a cryptic nuclear localization signal that allows it to move to the nucleus and initiate a number of gene programs, including activation of T-cells. Despite its physiological importance, CaN regulation at the molecular level is still poorly understood but differs significantly from that of the CaM-activated kinases.

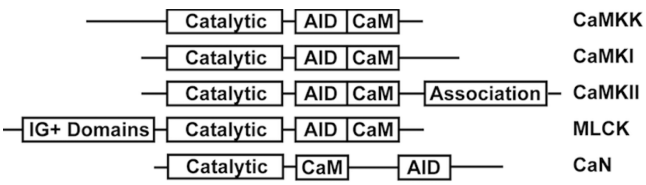

Figure 1. Domain ordering of CaM-activated kinases compared to the domain ordering of CaN.

As a result of its role in activating the immune system, CaN is the target of immunosuppressant drugs.[12] These drugs, FK506 (tacrolimus) and cyclosporin, each bind first to the prolyl isomerases FKBP12 and cyclophilin, respectively. These drug:prolyl isomerase complexes then bind CaN, inhibiting the phosphatase.[13,14] Immunosuppressant drugs are known to have numerous side effects, including serious ones such as nephrotoxicity.[15,16] There is the possibility that some side

Received: April 17, 2013
Revised: October 5, 2013
Published: November 6, 2013

effects arise as a result of inhibition of the prolyl isomerases in addition to CaN. Understanding the molecular details of how CaN is activated by CaM could lead to the identification of currently unknown interactions that could be targeted with drugs.

CaN is a heterodimer composed of an A-chain and a B-chain. The ~60 kDa A-chain houses a catalytic domain, a B-chain binding helix, a regulatory domain (RD), an autoinhibitory domain (AID), and a C-terminal tail (CT).[17] The CaM binding region (CaMBR) is a 24-residue stretch within the regulatory domain (Figure 2). The 19 kDa B-chain is structurally homologous to CaM and is capable of binding four calcium ions.[18] There are three dominant CaN isoforms: the neuron specific αCaN, ubiquitous βCaN, and the testes specific γCaN.[19] Here, we discuss αCaN, and further use of CaN will refer to αCaN.

Similar to the CaM-activated kinases, CaN has an AID that blocks the catalytic site until calcium-loaded CaM binds.[19] However, unlike the kinases, CaN's CaM binding region is N-terminal to the AID and separated from it by 52 residues (Figure 1). CaN's CaMBR is located in the regulatory domain (RD) of CaN (Figure 2). Trypsin digests by Manalan and Klee[20] and other hydrolysis experiments by Yang and Klee[19] demonstrated that the RD is readily hydrolyzed, showing that it is flexible and accessible in nature. In the structure of full-length CaN, the electron density for the RD and C-terminal tail (CT) is missing, suggesting that these regions are highly mobile.[21] Additionally, Romero and Dunker[22] noted that the sequence of the RD gave it the potential to be disordered. The trypsin digests performed by Manalan and Klee also suggested that the RD of CaN undergoes a large conformational change upon CaM binding as the highly unprotected RD becomes protected from trypsin digest when CaN is preincubated with CaM.[20] Surprisingly, this potentially disordered RD is 95 residues long, whereas the CaM binding site is ~24 residues long, suggesting that CaM binding induces conformational changes outside of the CaMBR.

Work by Rumi-Masante et al. showed by hydrogen–deuterium exchange mass spectrometry and circular dichroism spectroscopy that a fragment corresponding to CaN's RD, AID, and CT (RD–AID–CT) is disordered in the absence of CaM, though the AID is well-ordered in full-length, inactive CaN.[23] The RD portion of this fragment contains the CaM binding region and the 52 residues that separate it from the AID. Canonically, CaM's two lobes wrap around its target site and induce an α-helix in that sequence. How then does CaM activate CaN with its CaMBR and AID 52 residues apart and with those 52 residues disordered?

Rumi-Masante et al. also showed that upon CaM binding, ~50 residues within the RD become protected from H/D exchange and that the RD gains approximately 50 residues of α-helicity.[23] Approximately half of these residues reside in the CaMBR, while the remainder are C-terminal to the CaMBR, residing between it and the AID (Figure 2b). The high level of protection and α-helicity of the CaMBR when CaM is bound are expected given the very tight binding between CaM and CaN (K_D ~ 1pM) and the manner in which CaM typically binds its targets.[24] The level of protection and helicity in the region between the CaMBR and AID, suggested by RD protection in Manalan and Klee's CaN/CaM trypsin digests and confirmed by Rumi-Masante et al., suggests structuring on a scale larger than just the sequence CaM directly binds.[20,23]

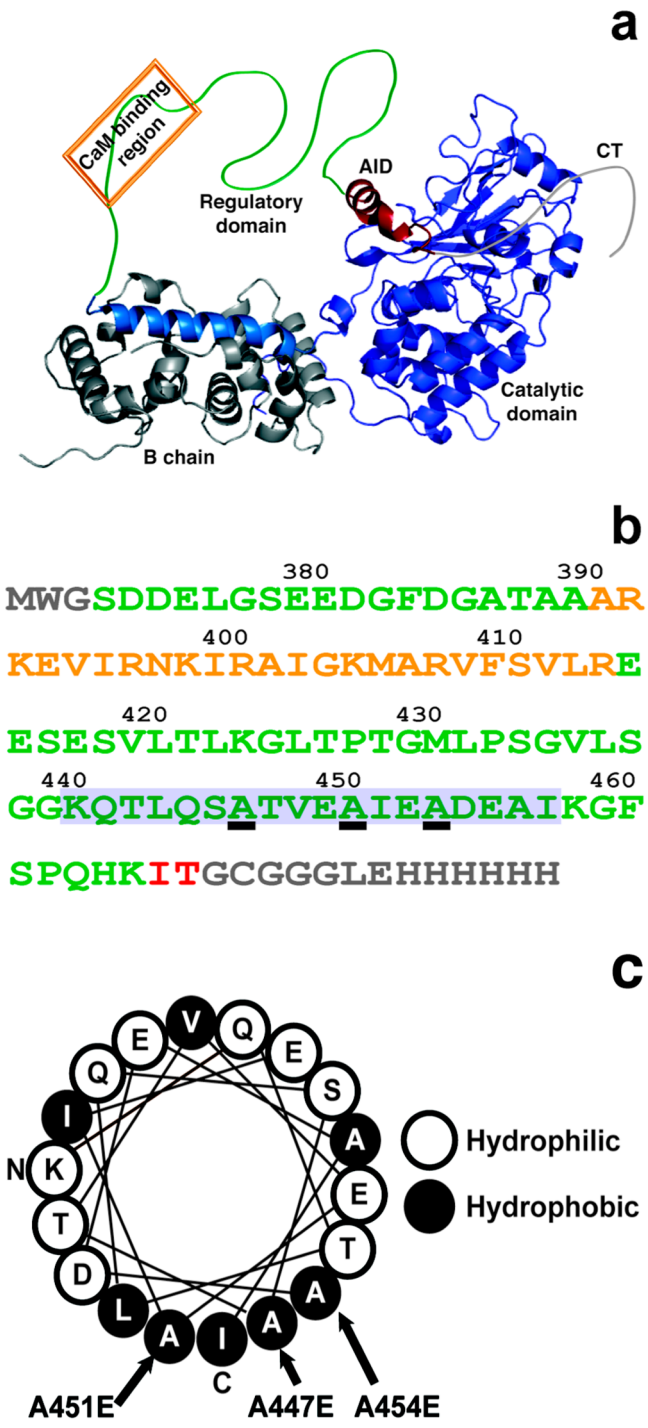

Figure 2. (a) Structure of CaN with domains highlighted (Protein Data Bank entry 1AUI).[21] (b) Sequence of the RD construct with the distal helical region highlighted by the blue region and the mutated alanine residues underlined. The RD is colored green, the CaMBR orange, the portion of AID red, and extraneous sequence gray. Extraneous sequence was added for the purpose of protein expression and purification. (c) Helical wheel projection of the distal helix. The alanine to glutamate mutations made on the hydrophobic face are indicated. N and C mark the N-terminal and C-terminal residues of the putative helix, respectively.

Examination of the protected area between the CaMBR and AID reveals that residues 441–459 could form an amphipathic α-helix (Figure 2c). It is unlikely that a helix in this region would be an extension of the helix formed at the CaMBR upon

dx.doi.org/10.1021/bi400483a | Biochemistry 2013, 52, 8643–8651

CaM binding as the region between the CaMBR and this proposed helix is populated with glycines and prolines, residues known to be unfavorable in α-helices (Figure 2b).[25] An amphipathic helix in this region would imply the need for the hydrophobic face of the helix to interact with another hydrophobic region; however, we know from Rumi-Masante et al. that the CaM-bound RD−AID−CT does not interact with the remainder of CaN and that the only regions in the RD−AID−CT to gain significant secondary structure upon CaM binding is the CaMBR and part of the region between it and the AID.[23] Therefore, we hypothesize that an amphipathic helix in the region between the CaMBR and AID would interact with the surface of the remainder of the RD:CaM complex when CaM is bound to the CaMBR of CaN. The end of this proposed helix is seven residues from the beginning of the AID. If it forms and folds back upon the RD:CaM complex when CaM binds the RD, this could provide the free energy necessary to remove the AID from the catalytic site. We will refer to this possible helix as the distal helix. In this work, we explore the nature and importance of the structure and function of this putative distal helix in the RD of CaN.

MATERIALS AND METHODS

Proteins, Peptide, and Buffer. Plasmid pETagHisCN containing the human αCaN A (with the N-terminal His_6 tag) and B1 genes, together forming αCaN, was obtained from Addgene (Cambridge, MA). This was transformed into *Escherichia coli* BL21(DE3) CodonPlus RIL cells (Agilent Technologies, La Jolla, CA) for expression. αCaN was purified on a Ni-NTA column followed by a CaM-Sepharose column (GE Healthcare, Piscataway, NJ). Human CaM was expressed from the pETCaMI vector in *E. coli* BL21(DE3) cells (Agilent Technologies) and purified on a 2-trifluoromethyl-10-aminopropyl phenothiazine-Sepharose column.[26] The 2-trifluoromethyl-10-aminopropyl phenothiazine-Sepharose was synthesized at the Center for Structural Biology Chemistry Core Facility at the University of Kentucky.

An *E. coli* codon-optimized gene for the human sequence RD construct was synthesized by Genscript (Piscataway, NJ). This was cloned into the pET303/CT-His vector that adds a C-terminal His_6 tag (Invitrogen, Carlsbad, CA) and cotransformed with pETCaMI for coexpression of the RD and CaM in *E. coli* BL21(DE3) cells. After expression, the RD was purified on a Ni-NTA column using a urea/thiourea gradient to remove CaM. The clarified RD−CaM lysate was run over a Ni-NTA column equilibrated in a 7 M urea/thiourea buffer [20 mM Tris (pH 7.5), 200 mM NaCl, 10 mM imidazole, 5 M urea, and 2 M thiourea]. Five column volumes (CV) of 7 M urea/thiourea buffer was added to the column, and the column was incubated at room temperature, while being shaken, for 30 min. The urea/thiourea concentration was decreased from 7 to 0.125 M by washing the column six times with 2.5 CV of urea/thiourea buffer that was diluted by half each time. The column was washed with 10 CV of 20 mM Tris (pH 7.5), 200 mM NaCl, and 10 mM imidazole to remove any remaining urea/thiourea buffer. The protein was eluted with 20 mM Tris (pH 7.5), 200 mM NaCl, 2 mM $CaCl_2$, and 250 mM imidazole and further purified with a CaM-Sepharose column.

A separate construct, RDc (Figure 3), was generated for fluorescence resonance energy transfer (FRET) measurements. This construct was expressed and purified following the same protocol described above for the RD construct. The fluorophore 5-({[(2-iodoacetyl)amino]ethyl}amino)-naphthalene-1-sulfonic acid (IAEDANS) was covalently coupled to the N-terminal cysteine following the manufacturer's protocol (Invitrogen). This forms a FRET pair with the C-terminal tryptophan in the RDc (Figure 3). Labeling efficiency was estimated from the IAEDANS absorbance at 336 nm using an extinction coefficient of 5700 M^{-1} and the tryptophan absorbance at 280 nm using an extinction coefficient of 5690 M^{-1} and correcting for fluorophore absorbance at that wavelength.

Figure 3. Sequence of the RDc construct used for the FRET studies. The cysteine to which the acceptor IAEDANS is covalently coupled and its donor tryptophan are underlined.

αCaN and RD mutants were generated using the Stratagene QuikChange II site-directed mutagenesis kit (Agilent Technologies) and purified as their wild-type counterparts. All expressed proteins had their identities confirmed via mass spectrometry. Protein concentrations were determined using the bicinchoninic acid assay.[27]

The pCaN peptide (sequence of ARKEVIRNKIRAIGKMARVFSVLR) corresponding to the CaM binding region in the RD of αCaN was purchased from Genscript. Modified p-RII (WGGDLDVPIPGRFDRRV[pS]VAAE), from the cAMP-dependent protein kinase regulatory subunit (type II), is the CaN substrate used in the phosphatase assays and was obtained from Atlantic Peptides (Scarborough, ME).[28] The N-terminal tryptophan was added for accurate determination of the peptide concentration using the absorbance at 280 nm, and the following two glycines were added to act as a linker between the tryptophan and remainder of the peptide. Both peptides were purified using reverse-phase high-performance liquid chromatography, and their identities were confirmed using mass spectrometry.

CD spectra were obtained using a buffer consisting of 20 mM Tris, 200 mM NaCl, and 2 mM $CaCl_2$ (pH 7.5). CD melts were obtained using a buffer consisting of 20 mM HEPES, 200 mM NaCl, and 2 mM $CaCl_2$ (pH 7.5). Phosphatase assays were performed in assay buffer consisting of 80 mM Tris (pH 7.5), 100 mM NaCl, 5 mM $MnCl_2$, 1 mM DTT, and 1 mM $CaCl_2$. All reagents used for these buffers were obtained from Sigma (St. Louis, MO) and were of the highest purity.

Circular Dichroism. CD spectra were recorded at 20 °C using a Jasco J-810 spectrapolarimeter equipped with a Peltier heating block. Samples containing each protein at 15 μM were placed in a 1 mm path-length cuvette, with reported spectra being the average of three scans at a scan speed of 50 nm/min. Errors are estimated to be no more than 3%. The thermal melts of the RD, CaM, and pCaN constructs were conducted with a heating rate of 1 °C/min and were monitored at a wavelength of 222 nm with reported melts being the average of five or six scans.

Fluorescence Resonance Energy Transfer. Fluorescence data were collected on an ISS K2 fluorometer with a Peltier heating block. Samples containing 8 μM RDc (labeled or unlabeled), with or without a 4-fold excess of CaM, were placed

dx.doi.org/10.1021/bi400483a | *Biochemistry* 2013, 52, 8643−8651

in 1 cm path-length quartz cuvettes. Tryptophan was excited at 295 nm using 8 μm slit widths. Emission spectra for both tryptophan and IAEDANS were recorded in the range of 320−530 nm using a 300 nm long-pass filter. Data were collected at temperatures ranging from 10 to 60 °C in 10 °C increments. FRET efficiencies were estimated from differences in tryptophan emission intensities and converted to distances using a Förster radius of 22 Å after correcting the FRET efficiency for the fraction of IAEDANS labeling.[29] Statistical significance was estimated using a two-tailed t test.

Phosphatase Assays. p-RII phosphatase assays were performed in assay buffer; 50 μL reaction mixtures contained 30 nM CaN or its mutant, 90 nM CaM, and 0−125 μM p-RII as a substrate. Reactions were initiated with p-RII and proceeded for 7 min at 30 °C. Reactions were terminated, and free phosphate was detected by addition of 100 μL of Biomol Green Reagent (Enzo Life Sciences) and incubation for 20 min and absorbance measured at 620 nm.

Phosphatase activity against the small molecule substrate p-nitrophenyl phosphate (pNPP) was also determined in assay buffer. pNPP was obtained from Sigma and was of highest purity available. Reaction mixtures contained 30 nM CaN or its mutant, 90 nM CaM, and 0−100 mM pNPP. The absorbance of the released p-nitrophenyl (pNP) was measured at 405 nm. Reaction rates were found to be linear out to 60 min. Data for kinetics analysis were collected at 30 min.

Each phosphatase assay was performed on protein from two different preparations and performed in triplicate for each protein. Kinetic constants were determined by fitting substrate versus initial velocity plots to the Michaelis−Menten equation using KaleidaGraph. Data were averaged over all assays for each protein, and errors were estimated from the standard deviations. The statistical significance was estimated using a two-tailed t test.

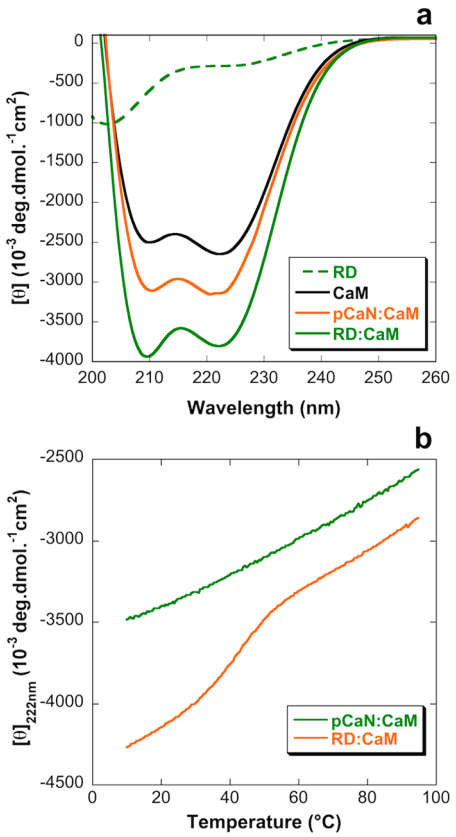

Figure 4. (a) Far-UV CD spectra recorded at 20 °C for the RD, CaM, pCaN complexed with CaM, and RD complexed with CaM. (b) Thermal melts following the CD signal at 222 nm from 10 to 95 °C for pCaN complexed with CaM and RD complexed with CaM.

RESULTS

The Secondary Structure of the RD:CaM Complex Is Similar to That of the RD−AID−CT:CaM Complex. To investigate CaM-induced structure and a possible distal helix in the region C-terminal to the CaMBR, we created a construct consisting of only the RD of CaN (Figure 2b). This new RD construct lacks the autoinhibitory domain and C-terminal tail (~50 residues) we had previously studied.[23] It was shown by Rumi-Masante et al. via CD spectroscopy and H/D exchange mass spectrometry (HXMS) that there was no detectable gain of structure in the AID or CT upon binding of CaM to the RD−AID−CT fragment.[23] To analyze the secondary structure of the RD, we obtained CD spectra of the RD alone. The spectrum is consistent with that of an unstructured polypeptide chain (Figure 4a).

An equimolar mixture of CaM and a 24-residue peptide corresponding to the CaMBR of CaN (pCaN) yields a spectrum with an increased α-helical content as compared to that of CaM alone, as is evident from the more negative minima of the CaM:pCaN complex at 208 nm and 222 nm, indicators of α-helix (Figure 4a). This increase in helicity is expected for CaM binding and inducing helix in its target. However, an equimolar mixture of CaM and the RD demonstrates that the RD:CaM complex has greater helical content than the pCaN:CaM complex (Figure 4a). These data are similar to those published by Rumi-Masante et al. for CaM, the pCaN:CaM complex, the RD−AID−CT fragment, and the RD−AID−CT:CaM complex.[23]

The CaM-Induced RD Structure Is Less Stable Than the pCaN:CaM Complex. Thermal melts of pCaN:CaM and RD:CaM complexes from 10 to 95 °C were obtained by monitoring the CD at 222 nm, the wavelength associated with minima in CD spectra caused by α-helices. The melt of the pCaN:CaM complex reveals no melting transitions, indicating that the pCaN:CaM complex is stable to at least 95 °C. The melt of the RD:CaM complex, however, shows a melting transition with a T_m of 42.4 ± 0.2 °C (Figure 4b). The major difference in sequence between the pCaN:CaM and RD:CaM complexes lies with the addition of the region C-terminal to the CaMBR (Figure 2b); thus, the melting transition seen in the RD:CaM complex is consistent with the melting of a helix in this region.

CaM Binding Brings the Termini of the RD Together. FRET data were collected for the RDc construct with an IAEDANS fluorophore covalently attached to the N-terminus just prior to the CaMBR, and a Trp near the C-terminus (Figure 3). Note that this construct is shorter than the RD construct employed in the rest of this work (Figure 2b). Ensemble average distances (r_{FRET}) for this FRET pair in the RDc bound to CaM at 20 and 50 °C are shown in Figure 5a. At 20 °C, the average distance between the fluorophores is ~10 Å, indicating that the two termini of RDc are relatively close to one another. At 50 °C, r_{FRET} has increased to ~16 Å, consistent with the putative distal helix having melted (Figure 4b). A two-tailed t test indicates that this ~6 Å increase is significant (p = 0.003).

dx.doi.org/10.1021/bi400483a | Biochemistry 2013, 52, 8643−8651

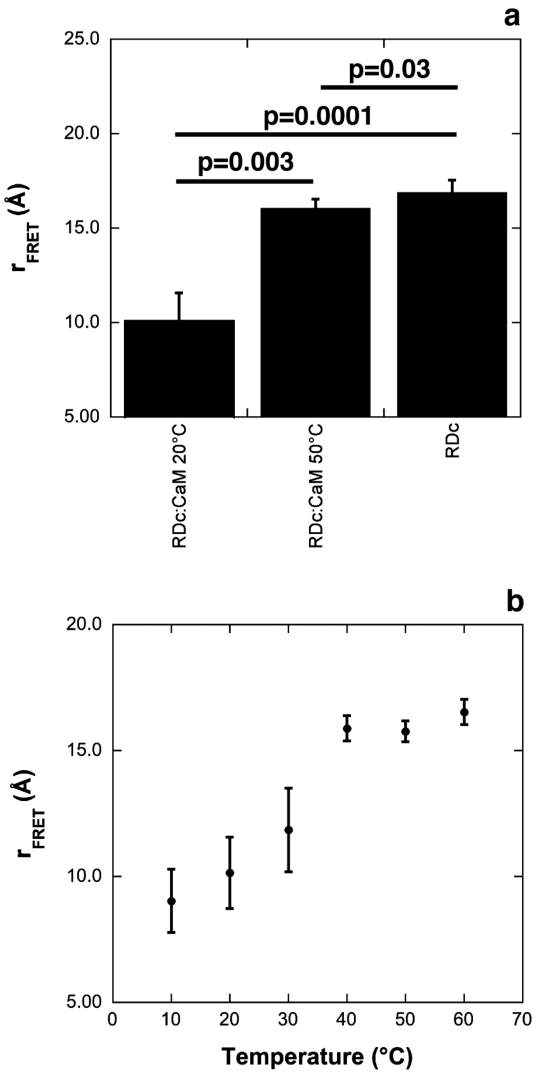

Figure 5. FRET distance data collected for the RDc labeled with IAEDANS. (a) Average distances between the Trp and IAEDANS FRET pair for the RDc in complex with CaM at 20 and 50 °C, and alone (averaged over all temperatures). (b) Temperature dependence of the estimated FRET distance for the labeled RDc bound to CaM.

Also shown in Figure 5a is the r_{FRET} for the unbound RDc averaged over all temperatures from 10 to 60 °C. The distance between the FRET pair did not vary with temperature for the unbound RDc. The r_{FRET} for the unbound RDc is only ∼1 Å larger than that for the RDc:CaM complex at 50 °C, a difference that is somewhat statistically significant (p = 0.03). The slightly shorter r_{FRET} for the RDc:CaM complex is likely due to CaM still being bound and the CaMBR being held in an α-helical conformation.

The behavior of r_{FRET} for the RDc:CaM complex as a function of temperature is shown in Figure 5b. Notably, there is a transition from an r_{FRET} of ∼9−12 Å at 10−30 °C to an r_{FRET} of ∼16 Å at 40−60 °C. This is similar to the melting transition observed via CD for the RD:CaM complex in Figure 4b. The FRET transition appears to occur between 30 and 40 °C (Figure 5b), somewhat lower than the T_m of 42.4 ± 0.2 °C determined from the CD data (Figure 4b).

Disruption of the Hydrophobic Face of the Putative Distal Helix Alters CaM-Induced Secondary Structure. The hydrophobic face of the putative distal helix is composed of a leucine, an isoleucine, and three alanines (Figure 2c). We created three RD mutants, RD-A447E, RD-A451E, and RD-A454E, that would disrupt the hydrophobic face but not necessarily prevent the formation of a helix as glutamates are charged but have high helical propensities.[25] The CD spectra of these mutants demonstrate that they are unstructured polypeptide chains similar to the wild-type RD (Figure 6a).

In contrast, addition of equimolar CaM to the RD mutants yields CD spectra that have helical content more similar to that of the pCaN:CaM complex, not that of the RD:CaM complex

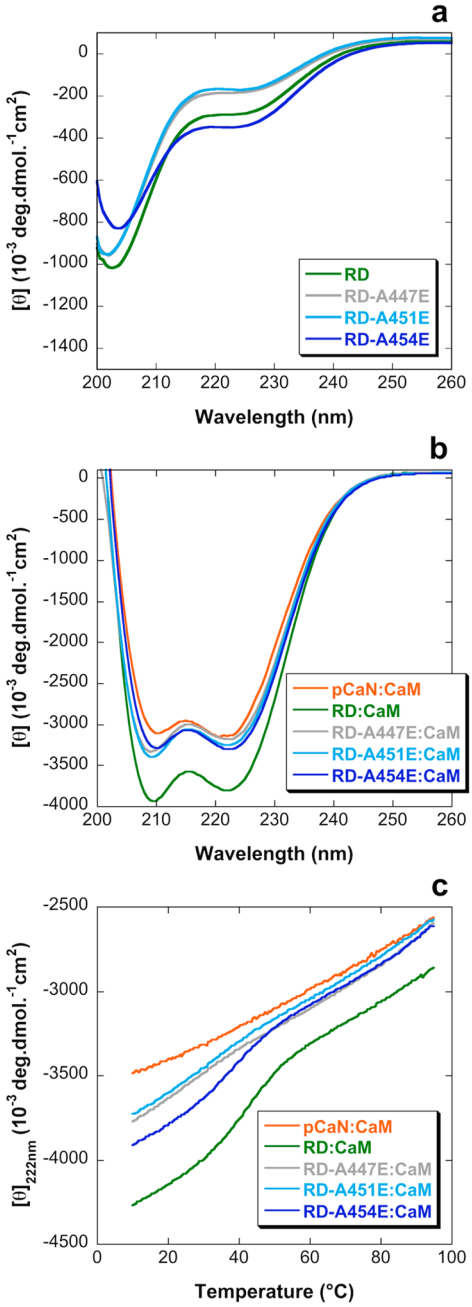

Figure 6. Far-UV CD spectra recorded at 20 °C for (a) RD, RD-A447E, RD-A451E, and RD-A454E and (b) pCaN, RD, RD-A447E, RD-A451E, and RD-A454E each complexed with CaM. (c) Thermal melts following the CD signal at 222 nm from 10 to 95 °C for pCaN, RD, RD-A447E, RD-A451E, and RD-A454E each complexed with CaM.

dx.doi.org/10.1021/bi400483a | *Biochemistry* 2013, 52, 8643−8651

Table 1. Kinetic Parameters of CaN and CaN Distal Helix Mutants for Dephosphorylation of the p-RII Peptide and of pNPP[a]

	p-RII peptide		pNPP	
	K_m (μM)	V_{max} (μmol min^{-1} mg^{-1})	K_m (mM)	V_{max} (μmol min^{-1} mg^{-1})
CaN	58 ± 12	2.67 ± 0.31	21.0 ± 3.5	1.59 ± 0.40
CaN-A447E	45 ± 8 (ns)	1.78 ± 0.46 (0.003)	38.8 ± 3.2 (4×10^{-6})	3.13 ± 1.13 (0.02)
CaN-A451E	44 ± 11 (ns)	1.38 ± 0.17 (5×10^{-6})	35.1 ± 7.4 (0.004)	2.31 ± 0.57 (0.02)
CaN-A454E	56 ± 15 (ns)	1.52 ± 0.29 (6×10^{-5})	29.4 ± 7.0 (0.003)	1.88 ± 0.25 (ns)

[a]The significance (p-value) relative to the wild-type value is given in parentheses. A lack of significance is denoted by ns.

(Figure 6b). The similarity of the spectra of the RD mutant:CaM complex to the spectrum of the pCaN:CaM complex indicates that the secondary structure in the region between the C-terminus and the CaMBR has been disrupted by the alanine to glutamate mutations. However, the spectra of the RD mutant:CaM complexes have slightly stronger 222 nm minima than the spectrum of the pCaN:CaM complex, with RD-A454E having the strongest, suggesting that they may have some residual distal helix.

Disruption of the Hydrophobic Face of the Putative Distal Helix Alters CaM-Induced Helix Stability. Thermal melts of RD mutants RD-A447E, RD-A451E, and RD-A454E with CaM were obtained by monitoring the CD at 222 nm from 10 to 95 °C as described above for the pCaN:CaM and RD:CaM complexes. Consistent with the CD spectra (Figure 6b), the RD mutants with CaM have more strongly negative signals than the pCaN:CaM complex at the beginning of the melt, with RD-A454E having the strongest (Figure 6c). This is indicative of more α-helix in the mutants with CaM than with the pCaN:CaM complex. However, all the mutants have signals approaching that of pCaN by the end of the melts. The wild-type RD:CaM complex has a stronger helical signal than any of the mutants with CaM or the pCaN:CaM complex, demonstrating its increased helicity in the region C-terminal to the CaMBR. Despite its weakened helical signal compared to that of the RD:CaM complex, the RD-A454E:CaM complex does have a melting transition. The T_m for this melting could not be obtained because of the absence of a native baseline for the melt of the RD-A454E:CaM complex. The weaker helical signal of the RD-A454E:CaM complex compared to that of the RD:CaM complex combined with the presence of a melting transition suggests that the RD-A454E mutant retains a partial distal helix, more than the other mutants, but the helix is diminished compared to that of the wild-type RD.

Disruption of the Hydrophobic Face of the Putative Distal Helix Diminishes CaM-Activated CaN Activity. To investigate the impact of the disruption of the hydrophobic face of the putative distal helix on CaN dephosphorylation kinetics, we introduced the same three alanine to glutamate mutations into full-length CaN as we did in the RD: CaN-A447E, CaN-A451E, and CaN-A454E. The CaM-induced activity of these mutants, as well as that of wild-type CaN, was assessed with a malachite green free phosphate assay using varying concentrations of the p-RII peptide from the cAMP-dependent protein kinase regulatory subunit (type II), a well-characterized CaN substrate.[28] Reactions were performed with a 1:3 CaN:CaM or CaN mutant:CaM ratio. Table 1 gives the kinetic parameters for CaN and the CaN mutants obtained under the conditions of our assay. The kinetic parameters for wild-type CaN are in good agreement with those obtained by Blumenthal et al.[28] The kinetic analysis reveals no significant change in K_m values for the CaN mutants compared to those of wild-type CaN (Table 1). On the other hand, there are significant decreases in V_{max} relative to that of the wild type. We also performed assays using the small molecule substrate pNPP. The results of the analysis of the kinetics of pNPP dephosphorylation are shown in Table 1. In this case, the K_m values of the mutants are increased. In addition, V_{max} values for A447E and A451E exhibit significant increases. These kinetic data indicate that the integrity of the hydrophobic face of this putative helix is important for CaN activity and impacts CaN's ability to bind the substrate.

DISCUSSION

In CaM-activated kinases, the CaMBR is directly C-terminal to the AID (Figure 1).[2,3] This proximity allows CaM to bind, causing the CaMBR to form an α-helix that removes the AID from the catalytic site, activating the kinase. Despite CaN having both a CaMBR and AID as the CaM-activated kinases do, CaM activation of CaN cannot occur in the same way as it does for the CaM-activated kinases given that the C-terminal end of the CaMBR is 52 residues N-terminal to the AID and these residues are disordered in the absence of CaM (Figure 1).[20,23,30] The intervening disordered residues seemingly prevent the removal of the AID from the active site when CaM binds at CaN's CaMBR.

Limited proteolytic digestions performed by Manalan and Klee and by Yang and Klee showing that the RD is readily degraded by proteases, missing RD and CT electron density in the CaN structure, and sequence analysis by Romero and Dunker all suggested that the RD is disordered.[20−22,30] Additionally, Manalan and Klee's trypsin digests of CaN preincubated with CaM showed that the RD became protected when CaM was bound to CaN, suggesting that the RD undergoes a conformational change upon CaM binding.[20] Rumi-Masante et al. used CD spectroscopy, hydrogen−deuterium exchange mass spectrometry, and limited tryptic digests to show that the RD−AID−CT fragment is disordered but gains structure upon CaM binding.[23] This structure includes the expected α-helix in the CaMBR, but it also includes one or more regions of helical structure somewhere between the end of the CaMBR and the beginning of the AID.

In this work, we investigated a construct of the RD alone. Previous hydrogen−deuterium exchange mass spectrometry and tryptic digestion data indicated that the structuring upon CaM binding occurred within the RD, and that the AID and CT were not involved.[23] Our CD spectra for the RD and the RD:CaM complex are comparable to those for the RD−AID−CT fragment and the RD−AID−CT:CaM complex described by Rumi-Masante et al., confirming that the α-helix gained upon CaM binding is in the RD, not the AID or CT.[23] We also performed thermal melts of pCaN:CaM and RD:CaM complexes. The thermal melt of the pCaN:CaM complex shows no cooperative melting transition as the pCaN:CaM complex is extremely stable (the K_D for the CaN:CaM complex is ~1 pM) and does not melt within the 10−95 °C range of our

thermal melts.[24] Therefore, the melting transition seen in the thermal melt of the RD:CaM complex must come from melting of helical structure in the RD outside of the CaMBR. Thus, CaM-induced helical content is in both the CaMBR and the remainder of the RD (Figure 4).

The CD spectra of the RD:CaM complex include changes in secondary structure for both the RD and CaM compared to the spectrum for CaM alone (Figure 4a). It is not possible to completely deconvolute the contributions of each protein in the complex. However, the RD:CaM complex appears to possess significantly more α-helical content than the pCaN:CaM complex. The difference between the spectra for these two complexes will be due to changes in secondary structure in the RD outside of the known CaM binding region, in addition to any within CaM induced by the RD. Given the marginal stability of the additional helical structure versus the high stability of the pCaN:CaM complex (Figure 4b), it seems unlikely that there are major changes to the CaM structure.

Further evidence of this folding of the RD onto CaM is provided by our FRET experiments. In these experiments, we employed a shortened RD construct called the RDc (Figure 3). This construct possesses a C-terminal Trp that acts as a FRET donor to an IAEDANS fluorophore covalently coupled to an N-terminal Cys. These fluorophores are located on average ~10 Å apart in the CaM-bound RDc at 20 °C (Figure 4). This distance is ~6 Å shorter than the ensemble average distance measured for the RDc alone and suggests that, in the complex, the N-terminus of the CaMBR is relatively close to the C-terminal end of the putative structured region. This supports the hypothesis that upon CaM binding the RD folds into a hairpinlike structure that provides sufficient free energy for the removal of the AID from the active site.

The temperature dependence of the estimated average FRET distances in the RDc:CaM complex (Figure 5b) appears to be similar to that observed for RD secondary structure in CD measurements (Figure 4b). However, the transition in the FRET data occurs between 30 and 40 °C, whereas the T_m estimated from the CD data is 42.4 ± 0.2 °C. The origin of this disparity is not clear. It is possible that interactions between the helical region outside of the CaMBR and CaM are disrupted at a temperature lower than that of helical region unfolding. We will be investigating this further in future studies.

Upon examination of the sequence in the region of the RD C-terminal to the CaMBR, identified by Rumi-Masante et al. as the region besides the CaMBR that gains structure upon CaM binding, we identified a portion that plots as an amphipathic helix on a helical wheel projection (Figure 2c).[23] From this, we proposed that an amphipathic helix in this region forms by folding its hydrophobic face onto the surface of the rest of the RD:CaM complex when CaM is bound to the CaMBR of CaN. We refer to this helix as the distal helix. Rumi-Masante et al. showed that the CaM-bound RD−AID−CT fragment does not interact with CaN's catalytic domain, B-chain binding helix, or B-chain, making the remainder of the RD:CaM complex the only other portion of CaN with which the distal helix could interact. Interaction of the distal helix with the remainder of the RD:CaM complex would create a hairpinlike chain reversal that could compensate for the 52 residues between the CaMBR and AID, allowing for the removal of the AID from the catalytic site, activating CaN. This helix would not be an extension of the CaMBR helix as the region between the CaMBR and this helix contains multiple glycines and prolines, residues known to be unfavorable in α-helices.

To test for the presence of the distal helix, we created three RD mutants: RD-A447E, RD-A451E, and RD-A454E (Figure 2). The alanine to glutamate mutations would disrupt the hydrophobic face of the helix but not necessarily prevent the formation of a helix as glutamates are charged but have high helical propensities.[25] CD spectra of these mutants were comparable to that of the wild-type RD, showing that they are disordered, but when CaM binds, the helical content gained is similar to that of the pCaN:CaM complex, not the RD:CaM complex (Figure 6a,b). This indicates that the mutations have caused a decrease in CaM-induced helical content.

Thermal melts of the RD mutants with CaM were similar to the thermal melt of the pCaN:CaM complex, demonstrating that the lost helical content is in the RD, but outside of the CaMBR (Figure 6c). Though the CD spectra and melts are closer to those of the pCaN:CaM complex than to those of the RD:CaM complex, the RD-A454E:CaM and RD-A447E:CaM complexes have higher apparent helical contents, as judged by the ellipticity at 222 nm, than the RD-A451E:CaM complex. The RD-A454E:CaM complex even has a visible melting transition, though a T_m could not be determined. As A451 is central to the distal helix, and A447 and A454 would be nearer the N- and C-terminal limits of the helix, mutation of the central alanine (A451) may disrupt the entire helix, whereas mutation of the alanines closer to the termini (A447 and A454) may still allow for partial formation of the distal helix. We also note that thermal melting of the RD showed that the distal helix's T_m is 42.4 ± 0.2 °C, very near the physiological body temperature of 37 °C, suggesting that it is not very stable.[31] Given this, the reduced helical content of the hydrophobic face mutants and the absence of this helix when CaM is not bound to CaN suggest that the helix requires that its hydrophobic face interact with the remainder of the RD:CaM complex for it to form.

Given the marginal stability of the putative distal helix (Figures 4b and 5b), we do not think the mutants that disrupt it would have a significant effect upon the binding of CaM to CaN. CaM binds to CaN with an affinity in the low picomolar range.[32] O'Donnell et al. have shown that CaM also binds to the pCaN peptide from βCaN with a K_D of ~1 pM.[24] This latter result suggests that almost all of the free energy of binding is due to interactions between CaM and its ~24-residue binding region in the RD of CaN. Contributions from the formation of the distal helix are unlikely to be detectable given the already very tight binding.

To investigate the importance of the distal helix in CaN dephosphorylation activity, we created the same mutations in full-length CaN as we did in the RD: CaN-A447E, CaN-A451E, and CaN-A454E. Performing p-RII peptide/malachite green free phosphate assays on CaM-activated wild-type CaN and these mutants revealed increased apparent V_{max} values in the mutant CaNs compared to that of the wild type (Table 1). This might appear to be counterintuitive; the mutations disrupt formation of the distal helix and presumably allow the AID to bind at least partially in the active site. This should have the same effect as a competitive inhibitor and lead to reduced apparent K_m values. However, the p-RII peptide does not bind directly in the active site of CaN. Instead, the peptide binds primarily to a region on the B-chain−BBH interface known as the LxVP site.[28,33] Mutations within the distal helix region would not be expected to effect binding of p-RII to this site when CaN is in its calcium-loaded state.[30] Instead, we observe decreases in V_{max} for the three mutants. This observation is

dx.doi.org/10.1021/bi400483a | Biochemistry 2013, 52, 8643−8651

consistent with previous kinetic analyses of CaN activity against p-RII. Perrino et al. observed that the p-RII peptide bound to calcium-loaded CaN in the absence of CaM with the same K_m as to CaM-activated CaN.[34] Their measured V_{max}, however, was significantly lower for calcium-loaded CaN in the absence of CaM. CaM activation then does not affect the LxVP binding site,[34] but it is known to remove the AID from the active site.[23] Therefore, although its origins are not clear, our observation of low apparent V_{max} values for each mutant relative to that of wild-type CaN would be consistent with the AID still being able to occupy the active site.

We also performed kinetic assays using the small molecule substrate pNPP (Table 1). The results support our interpretation of the p-RII peptide dephosphorylation studies. In this case, the apparent K_m for each mutant is significantly higher than that of the wild type. This is what would be expected if the AID were blocking the active site, acting as a competitive inhibitor. Similar results were described by Sagoo et al.[35]

Interestingly, the V_{max} values for the A447E and A451E mutants are higher than that of the wild type (Table 1; the V_{max} for the A454E mutant is not significantly different from that of the wild type). An increase in CaN activity against pNPP has previously been observed in the presence of the immunosuppressant cyclosporin,[36] but it is not at all clear why our mutants would have this effect.

These alterations in kinetic parameters show that proper formation of the distal helix is important for CaN dephosphorylation activity. It is of note that while the mutants diminish CaN activity, they do not abolish it. The kinetic data for the three CaN mutants suggest that the AID can bind the active site even in the presence of CaM. However, the residual activity suggests that in the CaM-bound CaN mutants AID binding in the active site is not as tight as it is in wild-type CaN without CaM. This could be due to residual distal helix in the mutants or to the CaM-induced helical conformation of the CaMBR shortening the reach of the RD sufficiently to weaken binding even in the absence of distal helix formation.

On the basis of our mutation studies, we have shown that the distal helix is comprised of at least eight residues if A447 and A454 are considered to be the bounds of the helix. However, trypsin digest work by Rumi-Masante et al. showed that both K441 and K459 are protected from digestion, suggesting that the distal helix may extend from residue 441 to 459, beyond the limits suggested by our mutations (Figure 2b).[23] This gives an ~19-residue helix, which is consistent with the increase in helical content seen in the region between the CaMBR and AID by Rumi-Masante et al. This is also consistent with our helical wheel projection (Figure 2c).

We have shown that disruption of the hydrophobic face of the putative distal helix diminishes the helical content in this region and reduces CaN's affinity for the substrate. Residual CaN activity when the hydrophobic face of the distal helix is disrupted may be due to residual helicity of the distal helix. In light of the importance of the distal helix for CaN activity, we propose the following model for CaN activation by CaM. When CaM binds to the CaMBR in the RD of CaN, a stretch of residues N-terminal to the AID forms an amphipathic α-helix, which we have termed the distal helix. The hydrophobic face of the distal helix must interact with another hydrophobic region on the remainder of the RD:CaM complex to form. This interaction creates a hairpinlike chain reversal in the RD that compensates for the 52 residues between the CaMBR and AID and allows the AID to be removed from CaN's catalytic site when CaM binds, activating CaN. Notably, Ye et al. recently published a model for CaM-activated CaN that seems to suggest a helix in the same region of the RD as our proposed distal helix.[37]

The distal helix region identified in this work is not very stable, having a T_m of ~42 °C. However, its formation appears to be important for full activation of CaN by CaM. This region is then a putative target for small molecule inhibitors of CaN. Such inhibitors could represent lead compounds in the development of a new generation of immunosuppressant drugs. Drugs that prevent formation of the distal helix would be an improvement over the existing immunosuppressant drugs FK506 and cyclosporin in that they would not bind to and inhibit prolyl isomerases in the process of inhibiting CaN,[13] potentially reducing the severity of side effects.

AUTHOR INFORMATION

Corresponding Author

*E-mail: trevor.creamer@uky.edu. Phone: (859) 323-6037. Fax: (859) 257-2283.

Funding

T.B.D. was supported by a Predoctoral Fellowship from the American Heart Association (11PRE7020001). This work was supported by a grant from the National Science Foundation (MCB-0843551) to T.P.C. The Center for Structural Biology Chemistry Core Facility at the University of Kentucky is supported in part by funds from National Center for Research Resources Grant P20 RR020171.

Notes

The authors declare no competing financial interest.

ACKNOWLEDGMENTS

We thank Professor Anthony Persechini (University of Missouri at Kansas City, Kansas City, MO) for providing the pETCaMI expression vector, Farah El Najjar for preliminary work with an RD−AID−CT construct, and Stacy Webb for creation of the CaN mutations.

ABBREVIATIONS

CaN, calcineurin; CaM, calmodulin; CaMBR, calmodulin binding region; RD, calcineurin's regulatory domain; AID, calcineurin's autoinhibitory domain; BBH, calcineurin's B-chain binding helix; CaMKI, calmodulin kinase I; CaMKII, calmodulin kinase II; CaMKK, calmodulin kinase kinase; MLCK, myosin light chain kinase; NFAT, nuclear factor activating T-cells; pCaN, peptide corresponding to the calmodulin binding region in calcineurin; p-RII, phosphorylated peptide from the regulatory domain of cyclic AMP kinase; pNPP, *p*-nitrophenyl phosphate; IAEDANS, 5-({[(2-iodoacetyl)amino]ethyl}-amino)naphthalene-1-sulfonic acid; CD, circular dichroism; FRET, fluorescence resonance energy transfer.

REFERENCES

(1) Yap, K. L., Kim, J., Truong, K., Sherman, M., Yuan, T., and Ikura, M. (2000) Calmodulin target database. *J. Struct. Funct. Genomics 1*, 8−14.

(2) Swulius, M. T., and Waxham, M. N. (2008) Ca^{2+}/calmodulin-dependent protein kinases. *Cell. Mol. Life Sci. 65*, 2637−2657.

(3) Soderling, T. R. (1999) The Ca-calmodulin-dependent protein kinase cascade. *Trends Biochem. Sci. 24*, 232−236.

(4) Wang, J. H., and Desai, R. (1976) A brain protein and its effect on the Ca^{2+}- and protein modulator-activated cyclic nucleotide phosphodiesterase. *Biochem. Biophys. Res. Commun. 72*, 926−932.
(5) Klee, C. B., and Krinks, M. H. (1978) Purification of cyclic 3′,5′-nucleotide phosphodiesterase inhibitory protein by affinity chromatography on activator protein coupled to Sepharose. *Biochemistry 17*, 120−126.
(6) Watterson, D. M., and Vanaman, T. C. (1976) Affinity chromatography purification of a cyclic nucleotide phosphodiesterase using immobilized modulator protein, a troponin C-like protein from brain. *Biochem. Biophys. Res. Commun. 73*, 40−46.
(7) Rusnak, F., and Mertz, P. (2000) Calcineurin: Form and function. *Physiol. Rev. 80*, 1483−1521.
(8) Ermak, G., Morgan, T. E., and Davies, K. J. (2001) Chronic overexpression of the calcineurin inhibitory gene DSCR1 (Adapt78) is associated with Alzheimer's disease. *J. Biol. Chem. 276*, 38787−38794.
(9) Hoeffer, C. A., Dey, A., Sachan, N., Wong, H., Patterson, R. J., Shelton, J. M., Richardson, J. A., Klann, E., and Rothermel, B. A. (2007) The Down syndrome critical region protein RCAN1 regulates long-term potentiation and memory via inhibition of phosphatase signaling. *J. Neurosci. 27*, 13161−13172.
(10) Chakraborti, S., Das, S., Kar, P., Ghosh, B., Samanta, K., Kolley, S., Ghosh, S., Roy, S., and Chakraborti, T. (2007) Calcium signaling phenomena in heart diseases: A perspective. *Mol. Cell. Biochem. 298*, 1−40.
(11) Vega, R. B., Bassel-Duby, R., and Olson, E. N. (2003) Control of cardiac growth and function by calcineurin signaling. *J. Biol. Chem. 278*, 36981−36984.
(12) Rao, A., Luo, C., and Hogan, P. G. (1997) Transcription factors of the NFAT family: Regulation and function. *Annu. Rev. Immunol. 15*, 707−747.
(13) Li, H., Rao, A., and Hogan, P. G. (2011) Interaction of calcineurin with substrates and targeting proteins. *Trends Cell Biol. 21*, 91−103.
(14) Grigoriu, S., Bond, R., Cossio, P., Chen, J. A., Ly, N., Hummer, G., Page, R., Cyert, M. S., and Peti, W. (2013) The molecular mechanism of substrate engagement and immunosuppressant inhibition of calcineurin. *PLoS Biol. 11*, e1001492.
(15) Hesselink, D. A., Bouamar, R., and van Gelder, T. (2010) The pharmacogenetics of calcineurin inhibitor-related nephrotoxicity. *Ther. Drug Monit. 32*, 387−393.
(16) Krejci, K., Tichy, T., Bachleda, P., and Zadrazil, J. (2010) Calcineurin inhibitor-induced renal allograft nephrotoxicity. *Biomedical papers of the Medical Faculty of the University Palacký, Olomouc, Czechoslovakia 154*, 297−306.
(17) Hubbard, M. J., and Klee, C. B. (1989) Functional domain structure of calcineurin A: Mapping by limited proteolysis. *Biochemistry 28*, 1868−1874.
(18) Stemmer, P. M., and Klee, C. B. (1994) Dual calcium ion regulation of calcineurin by calmodulin and calcineurin B. *Biochemistry 33*, 6859−6866.
(19) Klee, C. B., Ren, H., and Wang, X. (1998) Regulation of the calmodulin-stimulated protein phosphatase, calcineurin. *J. Biol. Chem. 273*, 13367−13370.
(20) Manalan, A. S., and Klee, C. B. (1983) Activation of calcineurin by limited proteolysis. *Proc. Natl. Acad. Sci. U.S.A. 80*, 4291−4295.
(21) Kissinger, C. R., Parge, H. E., Knighton, D. R., Lewis, C. T., Pelletier, L. A., Tempczyk, A., Kalish, V. J., Tucker, K. D., Showalter, R. E., and Moomaw, E. W. (1995) Crystal structures of human calcineurin and the human FKBP12-FK506-calcineurin complex. *Nature 378*, 641−644.
(22) Romero, P., Obradovic, Z., and Dunker, A. K. (1997) Sequence Data Analysis for Long Disordered Regions Prediction in the Calcineurin Family. *Genome Informatics Workshop on Genome Informatics 8*, 110−124.
(23) Rumi-Masante, J., Rusinga, F. I., Lester, T. E., Dunlap, T. B., Williams, T. D., Dunker, A. K., Weis, D. D., and Creamer, T. P. (2012) Structural basis for activation of calcineurin by calmodulin. *J. Mol. Biol. 415*, 307−317.
(24) O'Donnell, S., Yu, L., Fowler, C. A., and Shea, M. A. (2011) Recognition of β-calcineurin by the domains of calmodulin: Thermodynamic and structural evidence for distinct roles. *Proteins 79*, 765−786.
(25) Chakrabartty, A., Kortemme, T., and Baldwin, R. L. (1994) Helix propensities of the amino acids measured in alanine-based peptides without helix-stabilizing side-chain interactions. *Protein Sci. 3*, 843−852.
(26) Charbonneau, H., Hice, R., Hart, R. C., and Cormier, M. J. (1983) Purification of calmodulin by Ca^{2+}-dependent affinity chromatography. *Methods Enzymol. 102*, 17−39.
(27) Smith, P. K., Krohn, R. I., Hermanson, G. T., Mallia, A. K., Gartner, F. H., Provenzano, M. D., Fujimoto, E. K., Goeke, N. M., Olson, B. J., and Klenk, D. C. (1985) Measurement of protein using bicinchoninic acid. *Anal. Biochem. 150*, 76−85.
(28) Blumenthal, D. K., Takio, K., Hansen, R. S., and Krebs, E. G. (1986) Dephosphorylation of cAMP-dependent protein kinase regulatory subunit (type II) by calmodulin-dependent protein phosphatase. Determinants of substrate specificity. *J. Biol. Chem. 261*, 8140−8145.
(29) Lakowicz, J. R. (2006) *Principles of fluorescence spectroscopy*, Springer-Verlag, Duesseldorf, Germany.
(30) Yang, S. A., and Klee, C. B. (2000) Low affinity Ca^{2+}-binding sites of calcineurin B mediate conformational changes in calcineurin A. *Biochemistry 39*, 16147−16154.
(31) Henkels, C. H., and Oas, T. G. (2005) Thermodynamic characterization of the osmolyte- and ligand-folded states of *Bacillus subtilis* ribonuclease P protein. *Biochemistry 44*, 13014−13026.
(32) Quintana, A. R., Wang, D., Forbes, J. E., and Waxham, M. N. (2005) Kinetics of calmodulin binding to calcineurin. *Biochem. Biophys. Res. Commun. 334*, 674−680.
(33) Roy, J., and Cyert, M. S. (2009) Cracking the phosphatase code: Docking interactions determine substrate specificity. *Sci. Signaling 2*, re9.
(34) Perrino, B. A., Ng, L. Y., and Soderling, T. R. (1995) Calcium regulation of calcineurin phosphatase activity by its B subunit and calmodulin. Role of the autoinhibitory domain. *J. Biol. Chem. 270*, 340−346.
(35) Sagoo, J. K., Fruman, D. A., Wesselborg, S., Walsh, C. T., and Bierer, B. E. (1996) Competitive inhibition of calcineurin phosphatase activity by its autoinhibitory domain. *Biochem. J. 320*, 879−884.
(36) Haddy, A., Swanson, S. K., Born, T. L., and Rusnak, F. (1992) Inhibition of calcineurin by cyclosporin A-cyclophilin requires calcineurin B. *FEBS Lett. 314*, 37−40.
(37) Ye, Q., Feng, Y., Yin, Y., Faucher, F., Currie, M. A., Rahman, M. N., Jin, J., Li, S., Wei, Q., and Jia, Z. (2013) Structural basis of calcineurin activation by calmodulin. *Cell. Signalling 25*, 2661−2667.